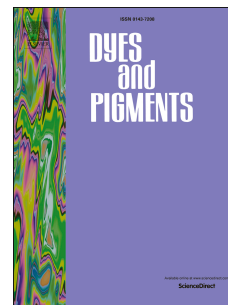


Accepted Manuscript

Synthesis, characterization and visible light activated fluorescence of azo caged aggregation-induced emission polymers

Bing Wu, Jiajia Shen, Wei Wang, Tianhao Xue, Yaning He



PII: S0143-7208(19)30726-0

DOI: <https://doi.org/10.1016/j.dyepig.2019.107569>

Article Number: 107569

Reference: DYPI 107569

To appear in: *Dyes and Pigments*

Received Date: 3 April 2019

Revised Date: 13 May 2019

Accepted Date: 19 May 2019

Please cite this article as: Wu B, Shen J, Wang W, Xue T, He Y, Synthesis, characterization and visible light activated fluorescence of azo caged aggregation-induced emission polymers, *Dyes and Pigments* (2019), doi: <https://doi.org/10.1016/j.dyepig.2019.107569>.

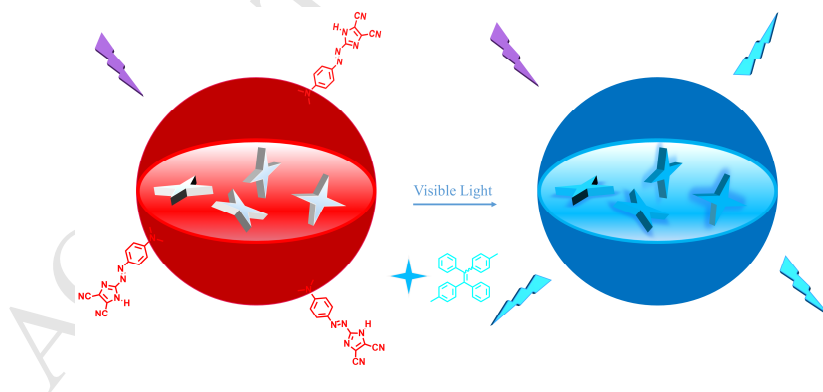
This is a PDF file of an unedited manuscript that has been accepted for publication. As a service to our customers we are providing this early version of the manuscript. The manuscript will undergo copyediting, typesetting, and review of the resulting proof before it is published in its final form. Please note that during the production process errors may be discovered which could affect the content, and all legal disclaimers that apply to the journal pertain.

Graphical Abstract

Synthesis, Characterization and Visible Light Activated Fluorescence of Azo Caged Aggregation-induced Emission Polymers

Bing Wu, Jiajia Shen, Wei Wang, Tianhao Xue and Yaning He*

Visible light activated fluorescence of imidazole-type azo caged aggregation-induced emission polymers was reported. The effect of azo contents on fluorescence intensity was studied, which revealed that only a small amount of imidazole-type azo groups could totally cage the strong AIE fluorescence of the polymers. Irradiated with visible light, azo chromophores could be photo bleached, leading to remarkable recovery of the blue fluorescence. Fluorescent patterns have been easily fabricated.



1 **Synthesis, Characterization and Visible Light Activated**
2 **Fluorescence of Azo Caged Aggregation-induced Emission**
3 **Polymers**

4 Bing Wu, Jiajia Shen, Wei Wang, Tianhao Xue and Yaning He*

5 Department of Chemical Engineering, Key Laboratory of Advanced Materials (MOE), Tsinghua
6 University, Beijing 100084, China

7 *Corresponding author: Tel. +86 01 62784561

8 E-mail: heyaning@mail.tsinghua.edu.cn

9
10 **Abstract**

11 Tetraphenylethylene (TPE) based aggregation-induced emission (AIE) polymers
12 containing different degrees of functionalization of photobleachable azo
13 chromophores were developed and their photophysical properties were explored. The
14 synthesized epoxy monomer derived from TPE core reacted with aniline to give the
15 precursor polymer, which confirmed typical AIE characteristics. Then through a
16 post-polymerization azo-coupling scheme, various contents of 2-phenylazo-4,
17 5-dicyanoimidazole groups were readily introduced into the TPE based epoxy
18 precursor polymer. Experimental results suggested that only a small amount of such
19 imidazole-type azo component could totally cage the intense AIE fluorescence of the
20 whole polymer due to the fluorescence resonance energy transfer process. By
21 exposure to visible light (450 nm), azo units could be photo bleached notably, thus
22 resulting in dramatic recovery of the blue fluorescence. Depending on this, visible

23 light induced fluorescent patterns were easily fabricated and erased, indicating that the
24 prepared azo caged AIE Polymers could be promising candidates for
25 anti-counterfeiting and optical information storage.

26 **Keywords:** Aggregation-induced emission; Azo caged; Tetraphenylethylene;
27 Visible light; Fluorescent polymer

28

29 1 Introduction

30 In recent years, stimuli-responsive caged fluorescent systems, whose emission is
31 quenched by a quencher and recovers upon cleavage of the quencher under certain
32 stimuli, have attracted considerable attention for their promising prospect in sensors,
33 optical recording devices, etc [1-4]. Anyway, traditional fluorescent compounds
34 generally suffer from the aggregation-caused quenching (ACQ) problem in
35 aggregated or solid state. In 2001, Tang's group proposed aggregation-induced
36 emission (AIE) first to address this thorny issue, leading to new insights into the
37 development of organic luminophores [5-16]. Due to AIEgens' good photostability
38 and high photobleaching resistance in aggregated state, caged AIE materials with
39 stimuli-responsive strategies have been extensively reported, which can be employed
40 in numerous applications ranging from chemical sensing to bioprobes and so on
41 [17-20]. Among diverse stimulus techniques, light is recognized to enjoy plenty of
42 unique advantages. For example, it is exceptionally convenient for light to adjust
43 irradiating position, intensity, beginning and ending time as well as specific
44 wavelengths. However, photoactivatable AIE systems are still rare. Tang et al. have

45 investigated a new caged fluorophore obtained by connecting a tetraphenylethylene
46 (TPE) derivative and a 2-nitrobenzyl group [21]. The caged compound can be
47 photoactivated and induced to emit strong cyan fluorescence by ultraviolet (UV)
48 exposure. Anyhow, UV light has very high energy, which can be damaging to
49 organisms and result in degradation for scores of macromolecules. To utilize lower
50 energy light resource such as visible light will be a much better choice [22]. In
51 particular, for the caged AIE compound, one fluorescent unit will be often linked with
52 one quencher, thus the fluorescence resonance energy transfer process can take place
53 well. However, one quencher may quench more than one fluorescent group. In terms
54 of this point, the caged AIE polymer may manifest better sensitivity to the stimuli.
55 Furthermore, AIE polymers hold much more advantages in practical applications for
56 their simple fabrication of large area films. Therefore, facile construction of
57 photoactivatable AIE polymers responding to visible light is reasonably important but
58 scarce.

59 Azo chromophores have been well known for their photoinduced reversible
60 isomerization upon irradiation with light at appropriate wavelength, which promises
61 potential in varying areas such as biological imaging, photoswitching, and many
62 others [23-31]. Besides photochromic behaviours, azo chromophores also have been
63 used as non-fluorescent energy acceptors, which can efficiently quench the
64 fluorescence of the system. We have found that azo groups could be effectively
65 bleached by enzyme or chemical reductant [32-34], causing great changes of both
66 ultraviolet-visible (UV-vis) absorption spectra and fluorescence emission spectra. In

67 addition to the above biological or chemical method, some kind of azo chromophore
68 has shown photobleachable performance with visible light actually [35]. On the basis
69 of this, a class of visible light triggered AIE-active polymers with various
70 photobleachable azo chromophore contents was synthesized and fully characterized in
71 this work. TPE was implemented as the fluorescent building block in the backbone of
72 epoxy based polymers owing to brief synthesis procedures and easy modifications.
73 Imidazole-type azo chromophores were chosen as photoquenching and
74 photobleaching sites. The photophysical properties of azo caged AIE polymers were
75 sufficiently discussed. Upon irradiation with the light at the wavelength of 450 nm,
76 the absorption band appearing in the visible range (λ_{\max} at 466 nm) ascribed to the π -
77 π^* electron transition of azo chromophores decreased noticeably, which was caused by
78 photobleaching without any addition of external reducing agents. Simultaneously, the
79 fluorescent emission of the polymer increased sharply. Furthermore, the fluorescent
80 pattern on the spin-coated film of the prepared azo caged AIE polymer was fabricated
81 and erased by exposure to visible light conveniently, which might be exploited in
82 anti-counterfeiting and optical information storage.

83 **2 Experimental Section**

84 **2.1 Materials and characterization**

85 The purification of tetrahydrofuran (THF) was accomplished by distillation with
86 metal sodium and benzophenone under argon atmosphere prior to use. Ultrapure
87 water with resistivity $> 18 \text{ M}\Omega\cdot\text{cm}$ was used in the experiments, which was obtained
88 from a Milli-Q water purification system. All other solvents and starting materials

89 were of analytical grade and purchased from commercial sources, which were directly
90 used without additional purification.

91 ^1H NMR and ^{13}C NMR spectra were conducted with a JEOL JNM-ECA 600 NMR
92 spectrometer by using deuterated chloroform (CDCl_3) or deuterated dimethyl
93 sulfoxide (DMSO-d_6) as the solvent and tetramethylsilane as the internal standard.

94 UV-vis absorption spectra were determined by using an Agilent 8453
95 spectrophotometer. Fourier transform infrared (FTIR) measurements were conducted
96 using an IRTracer-100 spectrometer (Shimadzu). Fluorescence emission spectra were
97 measured on a Hitachi F-7000 fluorescence spectrophotometer. The weight-average
98 molecular weight (M_w), the number-average molecular weight (M_n) and relative
99 molecular mass distribution (MWD) were determined on a gel permeation
100 chromatography (GPC) apparatus with THF as eluent at a flow rate of $1.0 \text{ mL}\cdot\text{min}^{-1}$.
101 Equipped with a refractive index detector and fitted with a PL gel 5 mm mixed-D
102 column, the instrument was calibrated by using linear polystyrene (PS) standards.

103 Photoirradiation (450 nm) was performed on a led curing system (IWATA UV-101D)
104 and the formed pattern was observed with a 365 nm UV lamp. The intensity of 450
105 nm visible light is about 150 and $500 \text{ mW}\cdot\text{cm}^2$ for the photobleaching of TPE-IZ-DC
106 with a DF of 2.5% and 38%, respectively. Mass spectra data were recorded on a
107 LCMS-IT/TOF (Shimadzu). Laser light scattering (LLS) measurements were
108 performed on an ALV/DLS/SLS-5022F spectrometer with a multi- τ digital time
109 correlator (ALV/LSE-5003) and a 17 mW solid-state laser ($\lambda = 632 \text{ nm}$) as the light
110 source.

111 2.2 Synthesis of **TPE-2OH**

112 To a solution of 4-hydroxybenzophenone (3.97 g, 0.02 mol) in dry THF (80 mL) was
113 added Zn dust (7.85 g, 0.12 mol). The mixture was stirred vigorously for a quarter of
114 an hour to cool to 0 °C. Into the above mixture was dropwise added titanium
115 tetrachloride (6.6 mL, 0.06 mol) and stirred in an ice water bath for 1 hour. Then it
116 was gradually heated to reflux under argon atmosphere for 24 hours. The reaction was
117 allowed to be cooled to room temperature and quenched with 10% K₂CO₃ aqueous
118 solution and the newly formed precipitate was removed. The residue was extracted
119 three times with 100 ml CH₂Cl₂, dried, filtered. After all of the solvent CH₂Cl₂ has
120 been evaporated under reduced pressure, the target product was further purified by
121 silica-gel column chromatography (300-400 mesh, eluent ethyl acetate / petroleum
122 ether 1:2 vol). White solid in 53% yield. ¹H NMR (600 MHz, CDCl₃), δ (TMS, ppm):
123 7.13-6.98 (m, 10H), 6.91-6.85 (m, 4H), 6.59-6.54 (m, 4H). ¹³C NMR (150 MHz,
124 CDCl₃), δ (TMS, ppm): 154.03, 144.28, 144.17, 139.82, 139.80, 136.79, 136.71,
125 132.87, 132.85, 131.51, 131.50, 127.82, 127.72, 126.38, 114.79, 114.71. MS(ESI) m/z:
126 [M-H]⁻ calcd C₂₆H₂₀O₂ 363.1391, found 363.1387.

127 2.3 Synthesis of **TPE-2EP**

128 A mixture of **TPE-2OH** (1 g, 2.74 mmol), epichlorohydrin (5.07 g, 54.8 mmol) and
129 isopropyl alcohol (35 ml) was sequentially added into 100 mL three-necked
130 round-bottom flask equipped with a magnetic stirrer and refluxed. Then 3.5 ml 20%
131 sodium hydroxide aqueous solution was dropwise added into the mixture over half an
132 hour. The reaction mixture stirred at reflux temperature under argon atmosphere for 5

133 hours. After cooling to room temperature, the mixture was poured into chloroform and
134 thoroughly washed with ultrapure water till neutrality. The combined organic layer
135 was dried over magnesium sulfate, filtered, and chloroform was removed by rotatory
136 evaporation under reduced pressure. The obtained crude product was further purified
137 by column chromatography over silica gel (300-400 mesh) using ethyl acetate /
138 petroleum ether (1:3 vol) as eluent. Yellow solid in 34% yield. ^1H NMR (600 MHz,
139 CDCl_3), δ (TMS, ppm): 7.12-7.07 (m, 6H), 7.03-7.01 (m, 4H), 6.92-6.90 (m, 4H),
140 6.64-6.63 (m, 4H), 4.14-4.11 (m, 2H), 3.89-3.87 (m, 2H), 3.32-3.30 (m, 2H),
141 2.89-2.87 (t, $J = 4.2$ Hz, 2H), 2.73-2.71 (m, 2H). ^{13}C NMR (150 MHz, CDCl_3), δ
142 (TMS, ppm): 156.98, 144.22, 139.83, 137.00, 132.69, 131.48, 127.83, 126.39, 113.81,
143 68.67, 50.21, 44.91. MS(ESI) m/z : [M] calcd $\text{C}_{32}\text{H}_{28}\text{O}_4$ 476.1982, found 476.1928.

144 2.4 Synthesis of **TPE-AN**

145 A mixture of **TPE-2EP** (1 g, 2.10 mmol) and phenylamine (0.1955 g, 2.10 mmol) was
146 added into 10 mL Schlenk flask equipped with a magnetic stirrer. After degassing and
147 recharging with argon, the solid was heated to be fused at 150 °C and kept one hour.
148 Subsequently, the reaction mixture was heated at 110 °C by stirring for another 24
149 hours. After the completion of the reaction, the resulting crude product was dissolved
150 into a minimal amount of dimethylformamide (DMF) and then precipitated with
151 excess petroleum ether to remove the unreacted **TPE-2EP** and phenylamine. The
152 product was isolated by filtration, vacuum dried at 65 °C over 24 hours for the use in
153 further post-polymerization azo-coupling scheme. White powder in 78% yield. ^1H
154 NMR (600 MHz, DMSO-d_6), δ (TMS, ppm): 7.12-7.08 (m, 8H), 6.97-6.93 (m, 4H),

155 6.86-6.82 (m, 4H), 6.71-6.67 (m, 6H), 6.59-6.51 (m, 1H), 5.33 (m, 1H), 5.15 (m, 1H),
156 4.01 (m, 2H), 3.83 (m, 4H), 3.68-3.66 (m, 1H), 3.55-3.53 (m, 1H), 3.43-3.40 (m, 1H),
157 3.30-3.27 (m, 1H). GPC: $M_n = 13000 \text{ g}\cdot\text{mol}^{-1}$; $M_w = 25700 \text{ g}\cdot\text{mol}^{-1}$; MWD = 1.98.

158 2.5 Synthesis of typical azo polymers **TPE-IZ-DC**

159 A series of azo polymers **TPE-IZ-DC** with different degrees of functionalization of
160 azo chromophores were synthesized through a post-polymerization azo-coupling
161 scheme. The brief procedures are as follows. To a solution of
162 2-amino-4,5-imidazoledicarbonitrile (0.319 g, 2.4 mmol) and 9 mL glacial acetic acid
163 was dropwise added 0.9 mL concentrated sulfuric acid at 0 °C. Then into the above
164 white mixture was dropwise added sodium nitrite (0.215 g, 3.12 mmol) in 0.9 mL of
165 water to give diazonium salts of 2-amino-4,5-imidazoledicarbonitrile. A mixture of
166 **TPE-AN** (100 mg) and 5 mL DMF was added into 25 mL round-bottom flask
167 equipped with a magnetic stirrer and cooled to 0 °C. And then, a certain amount of
168 diazonium salts was added dropwise into the above **TPE-AN** solution while the
169 temperature was maintained at 0 °C. The colourless solution turned to red immediately.
170 After being vigorously stirred overnight, the mixture was poured into excess saturated
171 brine. The pure product **TPE-IZ-DC** with specific azo content was filtered, vacuum
172 dried at 70 °C for 24 hours.

173 2.6 Preparation of the **TPE-IZ-DC** film

174 The substrates (quartz glass slides) were ultrasonically cleaned in sodium hydroxide
175 concentrated solution, ultrapure water and acetone, successively. And then they were
176 dried at 70 °C prior to use. A homogeneous solution of **TPE-IZ-DC** (50 mg) and

177 DMF (0.5 mL) was filtered with 0.25 μm filter. After that, it was spin-coated onto
178 substrates with a spin speed of 1500 rpm, followed by vacuum drying at 60 $^{\circ}\text{C}$ for 24
179 hours.

180 2.7 Visible light response of the **TPE-IZ-DC** film and fluorescent pattern 181 fabrication

182 **TPE-IZ-DC** films were vertically exposed to visible light (450 nm) at room
183 temperature to investigate the visible light response every thirty minutes with UV-vis
184 absorption spectrophotometer and fluorescence emission photometer. Fluorescent
185 patterns on the spin-coating films were fabricated by irradiating with the same light
186 source for 150 minutes through a photomask. Fluorescence images of the above
187 patterns were recorded under a 365 nm UV lamp.

188 3 Results and Discussion

189 3.1 Synthesis of azo caged AIE polymers **TPE-IZ-DC**

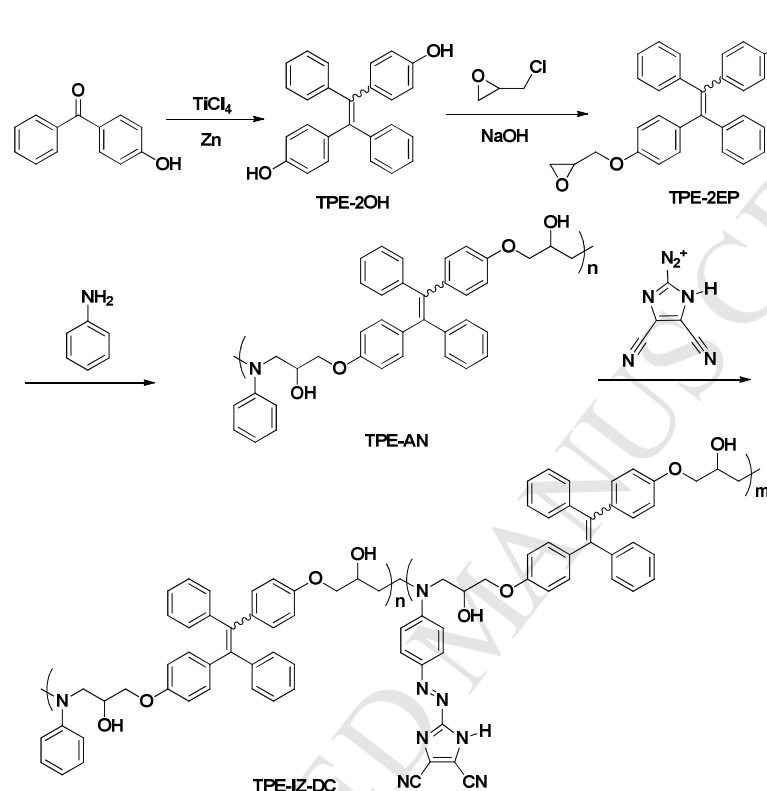
190 A set of visible light triggered AIE polymers **TPE-IZ-DC** containing different mole
191 fractions of azo groups was achieved and the synthetic route of target polymers
192 **TPE-IZ-DC** was illustrated in Scheme 1. According to the molecular design,
193 synthesis of azo caged polymers **TPE-IZ-DC** was facile with a four-step synthetic
194 approach. 1,2-bis(4-hydroxyphenyl)-1,2-diphenylethene (**TPE-2OH**), an iconic
195 AIEgen, was in a one-step preparation starting from 4-hydroxybenzophenone through
196 a McMurry coupling reaction. The TPE based epoxy compound (**TPE-2EP**) was
197 prepared by incorporating epoxy groups into **TPE-2OH**. Then synthesis of the
198 precursor polymer **TPE-AN** was done by the polycondensation of difunctional

199 epoxide and phenylamine monomers at relatively low temperature. The molecular
200 weight and molecular weight distribution of the linear polymer **TPE-AN** were
201 determined by GPC method and satisfying results were presented in Fig.S7. The
202 number-average molecular weight and relative molecular mass distribution of the
203 precursor polymer **TPE-AN** were $13000 \text{ g}\cdot\text{mol}^{-1}$ and 1.98, respectively. Finally, the
204 target polymers **TPE-IZ-DC** were synthesized by the post-polymerization
205 azo-coupling reaction between polymer **TPE-AN** and diazonium salts. The reaction
206 proceeded efficiently as expected and the final products **TPE-IZ-DC** displayed
207 glorious solubility in common organic solvents. Further details could be found in the
208 Experimental Section and Supporting Information.

209 ^1H NMR and ^{13}C NMR spectra suggested successful synthesis of all compounds,
210 which were included in the Supporting Information (Fig.S1 - 6). As could be seen
211 from ^1H NMR spectra of **TPE-AN** and **TPE-IZ-DC** (Fig.S5 and Fig.S6), the
212 incorporation of 2-phenylazo-4, 5-dicyanoimidazole parts has been identified by
213 combining information as follows. First, peak areas of protons at para-position of
214 anilino groups whose chemical shifts are around 6.55 ppm relatively reduced in the
215 whole low magnetic field corresponding to all aromatic rings. Second, the signal
216 newly appeared at 7.75 ppm was attributed to benzenoid protons at meta positions of
217 amino segments, which was caused by formation of electron-withdrawing azo groups.

218 We defined that degrees of functionalization (DFs) of azo chromophores were molar
219 ratios between 2-phenylazo-4, 5-dicyanoimidazole groups in the final polymer chain
220 and anilino pendants of the precursor polymer **TPE-AN**. Benefiting from efficient azo

221 coupling reaction, DFs could be controlled by selecting suitable amount of diazonium
 222 salts. The DFs have been estimated from ^1H NMR by comparing peak areas of
 223 protons of azo units and the others in the aromatic region.



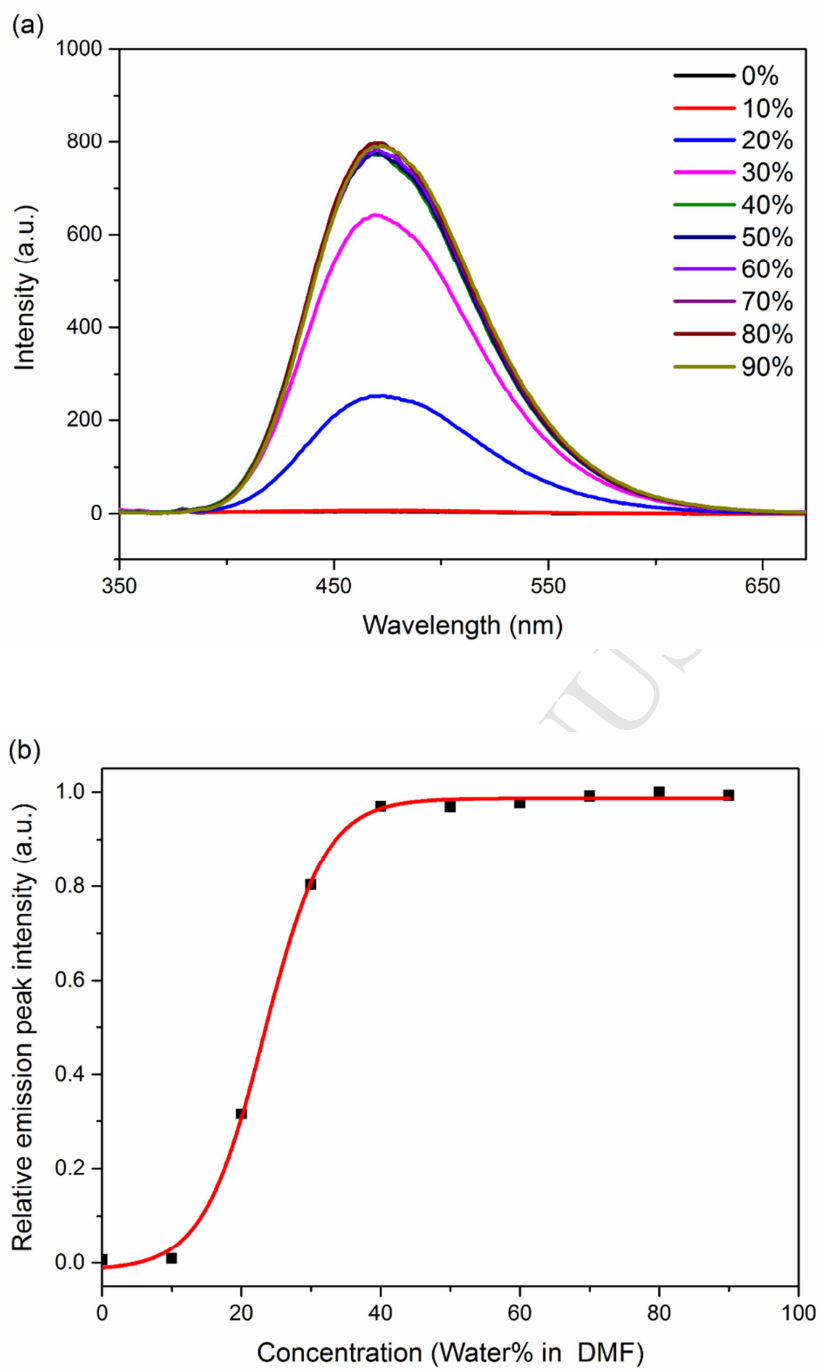
224

225 **Scheme 1.** Synthetic route of azo caged AIE polymers **TPE-IZ-DC**.

226 3.2 AIE effect of the precursor polymer **TPE-AN**

227 To explore AIE activity of the precursor polymer **TPE-AN**, fluorescence emission
 228 spectra were recorded in different ratios of water-DMF mixtures (Fig.1a). DMF was
 229 selected as the good solvent because **TPE-AN** could be resolved adequately and
 230 soluble with the poor solvent water at any proportion. When a little water was added
 231 to the DMF solution of **TPE-AN** (water proportion is lower than 10%), it was not
 232 emissive. The two spectra (0% and 10%) seemed to overlap each other. With

233 increasing the water percentage to 40%, blue fluorescence sharply enhanced, which
234 resulted from vast aggregation formation. After that, the maximum intensity remained
235 the same. The depict changes in fluorescence relative peak intensity (I/I_0) were shown
236 in Fig.1b. The relative intensity ratio (water contents are 90% and 0%, respectively)
237 was as high as 155, thus testifying its AIE nature. In the light of the restriction of
238 intramolecular motion (RIM) mechanism, aggregates of hydrophobic fluorescent
239 materials were increased with increasing poor solvent water. The aggregation of the
240 polymer was confirmed by Tyndall phenomenon and LLS. As water content was 90%,
241 an obvious Tyndall phenomenon emerged (Fig.S8), comparing with that in pure DMF.
242 LLS results also confirmed the formation of **TPE-AN** aggregates (Fig.S9). As water
243 content reach 98%, suspended solids were seen visually. As a result, **TPE-AN** could
244 be highly emissive in the aggregated state with maximum emission wavelength of 472
245 nm. Similar results were also found in the solid film of **TPE-AN** (Fig.S10). The
246 intense emission of the film also exhibited typical AIE feature. In addition, the
247 blueshift of emission peak position from aggregates to the solid film was about 5 nm.



248

249

250 **Fig. 1.** (a) Changes in fluorescence emission spectra of dilute solutions of **TPE-AN** in water-DMF mixtures with different water fractions.

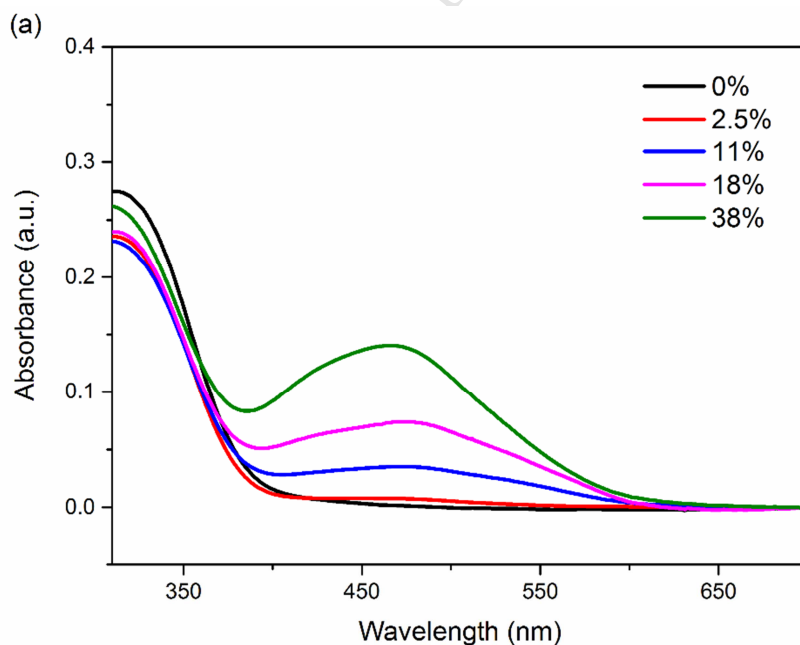
251 (b) Correlation between the relative emission peak intensity (I/I_0) at 472 nm of **TPE-AN** in water-DMF mixtures and water percentage.

252 Concentration of **TPE-AN**: 0.01 mg/mL; excitation wavelength: 340 nm.

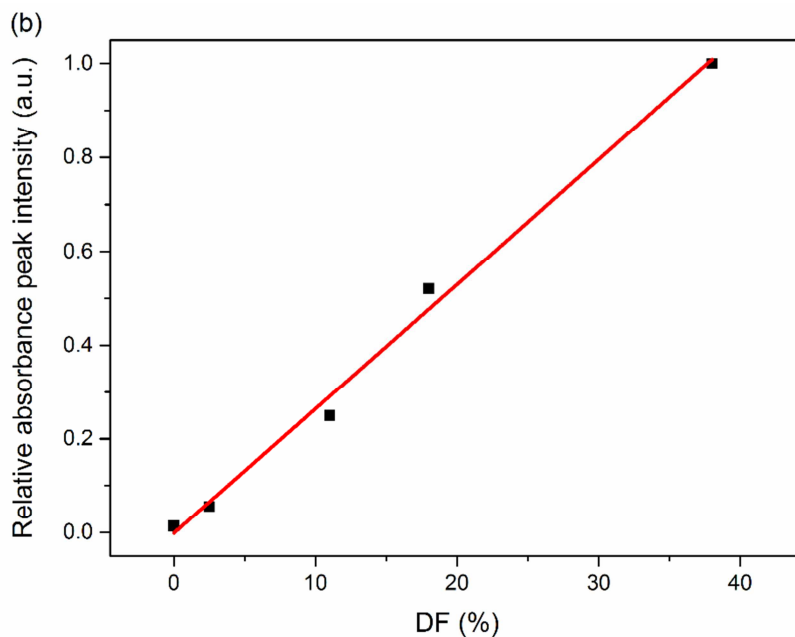
253 3.3 The relationship between absorption intensity of **TPE-IZ-DC** and

254 DFs

255 Besides fluorescence spectrometry, UV-vis absorption spectra of the polymer
256 **TPE-AN** was also recorded to study its optical property, corresponding to
257 **TPE-IZ-DC** with 0% DF, the black line in Fig.2a. No absorption peaks appeared in
258 the visible region for **TPE-AN**. For imidazole-containing polymers **TPE-IZ-DC** with
259 other DFs, they exhibited significant absorption ranging from 370 nm to 600 nm in
260 line with expectations, which also confirmed the introduction of heteroaromatic azo
261 moieties into polymer chains of **TPE-AN** successfully. The absorption maxima
262 appearing at 466 nm resulted from π - π^* electron transition of pseudo-stilbene type azo
263 chromophores. Fig.2b showed that the absorption maxima of **TPE-IZ-DC** in
264 water-DMF mixtures with 90% water fraction increased with the DFs.



265

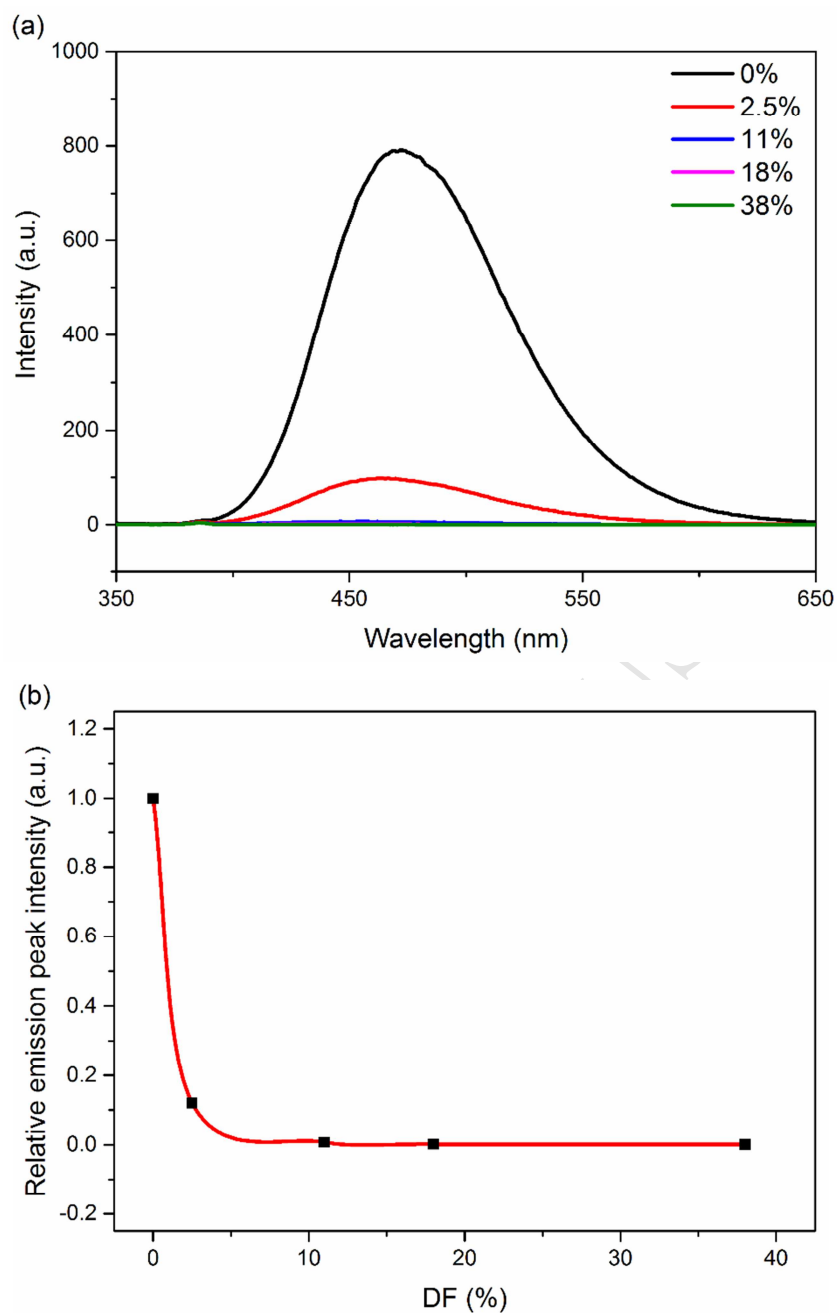


266

267 **Fig. 2.** (a) Changes in UV-vis absorption spectra of dilute solutions of **TPE-IZ-DC** with different DFs in water-DMF mixtures (90% water
 268 fraction). (b) Correlation between the relative absorption peak intensity (I/I_0) at 466 nm of **TPE-IZ-DC** and DFs in water-DMF mixtures
 269 (90% water fraction). Concentration of **TPE-IZ-DC**: 0.01 mg/mL.

270 3.4 Fluorescence quenching effect of **TPE-IZ-DC**

271 Since the absorption band of azo units almost covered all of emission region of TPE
 272 components proved in Fig.S11, fluorescence resonance energy transfer process would
 273 work and fluorescence of the polymers **TPE-IZ-DC** would be faded (Fig.3a). To
 274 verify the quenching efficiency, the influence of azo contents on fluorescence
 275 intensity was investigated. Fig.3b gives the curve of relative emission peak intensity
 276 at 472 nm of azo-containing polymers **TPE-IZ-DC** in water-DMF mixtures with 90%
 277 water fraction vs. DFs. It turned out as expected that the maximum value of emission
 278 intensity apparently decreased almost one order of magnitude by only 2.5% azo
 279 contents, implying excellent quenching efficiency of fluorescence.

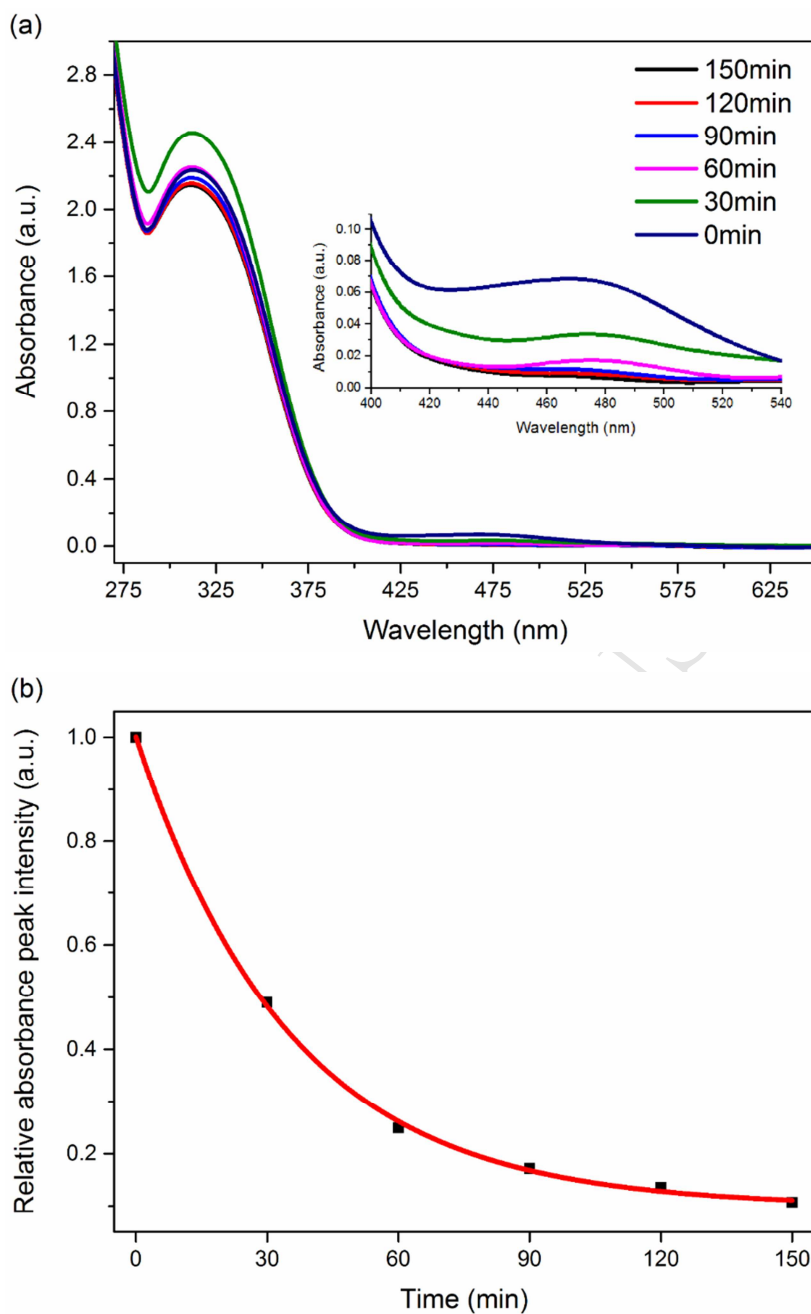


280

281

282 **Fig. 3.** (a) Changes in fluorescence emission spectra of dilute solutions of **TPE-IZ-DC** with different DFs in water-DMF mixtures (90%283 water fraction). (b) Correlation between the relative emission peak intensity (I/I_0) at 472 nm of **TPE-IZ-DC** in water-DMF mixtures (90%284 water fraction) and DF. Concentration of **TPE-IZ-DC**: 0.01 mg/mL; excitation wavelength: 340 nm.285 **3.5 Visible light response of the TPE-IZ-DC film**286 The epoxy based polymers **TPE-IZ-DC** had satisfactory thermal stability, good

287 transparency and favourable film-forming property. On the grounds of these,
288 **TPE-IZ-DC** films were obtained using the spin-coating method and visible light
289 response over different durations of light irradiation was measured by UV-vis
290 absorption spectra at first, as described in Fig.4. Given the convenience of
291 photobleaching, azo amount in the polymer was set at 2.5%. It has been demonstrated
292 that absorption maxima at 469 nm of the **TPE-IZ-DC** film reduced prominently under
293 continuous irradiation at the wavelength of 450 nm. Within only 30 minutes,
294 absorption intensity of residual azo functional groups was rapidly lost approximately
295 50%. After illumination for 150 minutes, it was only ninth of the originally state,
296 indicating a sensitive response to visible light as well as a high signal-to-noise ratio.
297 For pseudo-stilbene type azo chromophores, cis state is unstable and will rapidly relax
298 to the trans form. As shown in Fig.5, the absorption intensity at 469 nm from
299 **TPE-IZ-DC** decreased with the increase of irradiation time and the absorption peak
300 of **TPE-IZ-DC** upon irradiation was not recoverable at all even though we left the
301 film in the dark for a long time or heated. Besides, the irreversible color change of the
302 film was easily seen from red to almost colorless with the naked eye. It should be
303 considered that azo chromophores ultimately disappeared by photobleaching instead
304 of photoisomerization. FTIR spectra were also used to prove this photobleaching
305 process. As presented in Fig.S12, several characteristic peaks in FTIR spectra
306 assigned to absorption bands of **TPE-IZ-DC** (DF = 38%) decreased apparently, which
307 could be also postulated the photobleaching of azo chromophores after exposure to
308 450 nm light.



309

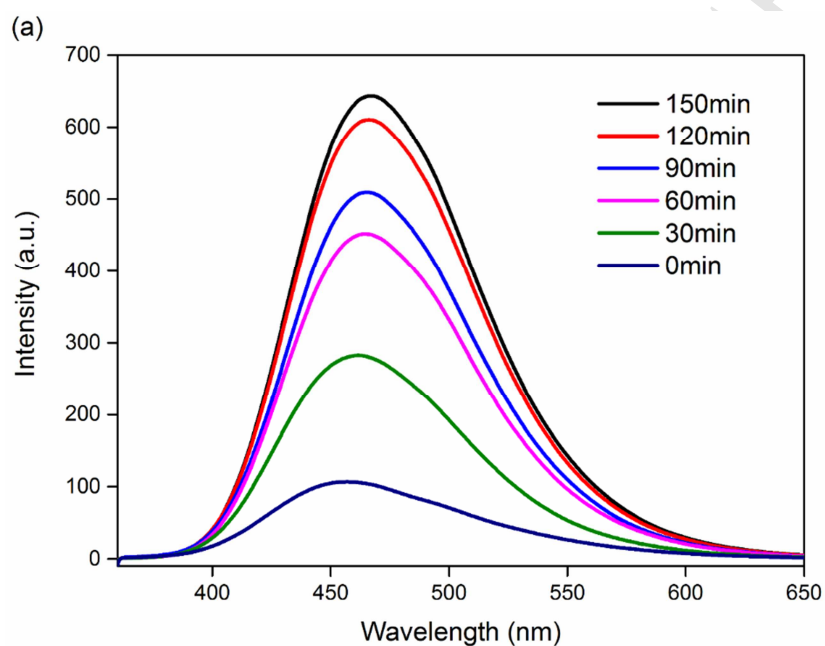
310

311 **Fig. 4.** (a) Time dependent absorption changes of the **TPE-IZ-DC** film irradiating with visible light at the wavelength of 450 nm. (b)

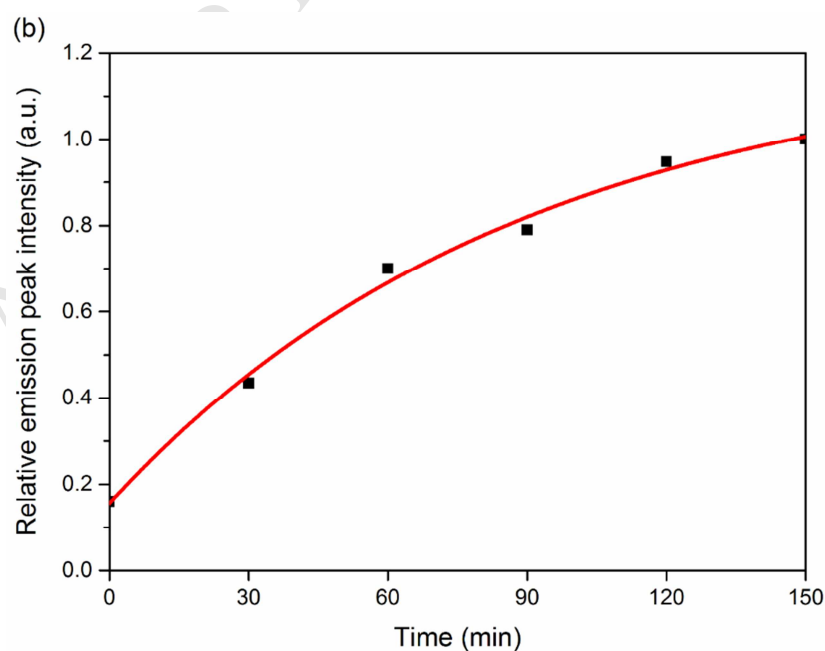
312 Correlation between the relative absorption peak intensity (I/I_0) at 469 nm of the **TPE-IZ-DC** film and exposure time.

313 As expected, changes of absorption intensity of the **TPE-IZ-DC** film greatly affected
 314 its fluorescence performance. Fig.5 clarified the blue fluorescence recovery after
 315 photobleaching by the same process of irradiation with visible light monitored by

316 fluorescence emission spectra. It could be found that characteristic emission definitely
317 increased as exposure time increased, in accordance with the UV-vis absorption
318 spectra. After irradiating the film with the same light source for 150 minutes,
319 photobleaching caused an increase in maximum emission intensity at 467 nm by more
320 than six times since fluorescence resonance energy transfer process did not work
321 anymore.



322

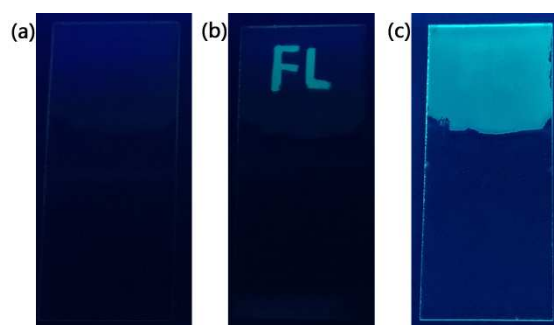


323

324 Fig. 5. (a) Time dependent fluorescence intensity changes of the **TPE-IZ-DC** film irradiating with visible light at the wavelength of 450
325 nm. (b) Correlation between emission peak intensity (I/I_0) at 467 nm of the **TPE-IZ-DC** film and exposure time.

326 3.6 The fluorescent pattern fabrication

327 The above results that visible light possessed the ability to efficiently bleach azo
328 chromophores and fluorescent emission was enhanced concomitantly impelled us to
329 make an attempt at fabricating fluorescent patterns by the mask method. These
330 observed patterns on the basis of photobleaching were transcribed from designed
331 photomasks. The feasibility and simplicity of the valid and powerful technique were
332 proved with an example. The mask was positioned onto the **TPE-IZ-DC** film, and
333 then the film was exposed to visible light using 450 nm light source for 150 minutes.
334 It was satisfying that the fluorescence of illumination field was brighter than its
335 surroundings. The letter pattern “FL” as a representative emerged as displayed in
336 Fig.6. After further irradiation, the pattern was almost completely erased. Due to this
337 successful demonstration, large-area or/and complicated patterns would be easily
338 tailored when films of the desired size and corresponding masks were applied, making
339 **TPE-IZ-DC** potentially suitable for optical information storage materials, antifake
340 materials and other application areas.



341

342 **Fig. 6.** The photographs of a piece of untreated film (a), the fluorescent pattern fabricated on exposed areas by visible light irradiation
343 process (b) and the pattern erasure after removing the mask under continuous irradiation (c) taken under a 365 nm UV lamp.

344 **4 Conclusions**

345 Azo caged aggregation-induced emission polymers were synthesized and their
346 fluorescence performance activated by visible light was fully characterized. The effect
347 of azo contents on fluorescence intensity was studied, which revealed that only a
348 small amount of imidazole-type azo groups could totally cage the strong AIE
349 fluorescence of the polymers due to the fluorescence resonance energy transfer
350 process. Irradiated with visible light, azo chromophores could be photo bleached,
351 leading to remarkable recovery of the blue fluorescence. Visible light induced
352 fluorescent patterns have been fabricated and erased, which indicated that the
353 prepared azo caged AIE Polymers could especially competitive in the material design
354 of anti-counterfeiting and optical information storage.

355 **Declaration of Interest**

356 The authors declare no competing financial interest.

357 **Acknowledgements**

358 The authors gratefully acknowledge financial support from the National Key R&D
359 Program of China (Grant No.2017YFA0701303), and the National Natural Science
360 Foundation of China (Grant Nos. 51873097 and 21674058).

361 **References**

362 [1] Bae J, McNamara LE, Nael MA, Mahdi F, Doerksen RJ, Bidwell III GL, et al.

- 363 Nitroreductase-triggered activation of a novel caged fluorescent probe obtained from methylene
364 blue. *Chem. Commun.* 2015;51(64):12787-90.
- 365 [2] Wei P, Li B, de Leon A, Pentzer E. Beyond binary: optical data storage with 0, 1, 2, and 3 in
366 polymer films. *J. Mater. Chem. C.* 2017;5(23):5780-6.
- 367 [3] Belov VN, Wurm CA, Boyarskiy VP, Jakobs S, Hell SW. Rhodamines NN: A Novel Class of
368 Caged Fluorescent Dyes. *Angew. Chem. Int. Ed.* 2010;49(20):3520-3.
- 369 [4] Chen S, Bian Q, Wang P, Zheng X, Lv L, Dang Z, et al. Photo, pH and redox multi-responsive
370 nanogels for drug delivery and fluorescence cell imaging. *Polym. Chem.* 2017;8(39):6150-7.
- 371 [5] Luo J, Xie Z, Lam JWY, Cheng L, Chen H, Qiu C, et al. Aggregation-induced emission of
372 1-methyl-1,2,3,4,5-pentaphenylsilole. *Chem. Commun.* 2001(18):1740-1.
- 373 [6] Mei J, Leung NL, Kwok RT, Lam JW, Tang BZ. Aggregation-induced emission: together we
374 shine, united we soar! *Chem. Rev.* 2015;115(21):11718-940.
- 375 [7] Wu Z, Pan K, Mo S, Wang B, Zhao X, Yin M. Tetraphenylethene-Induced Free Volumes for
376 the Isomerization of Spiropyran toward Multifunctional Materials in the Solid State. *ACS Appl.*
377 *Mater. Interfaces.* 2018;10(36):30879-86.
- 378 [8] Yang B, Zhang X, Zhang X, Huang Z, Wei Y, Tao L. Fabrication of aggregation-induced
379 emission based fluorescent nanoparticles and their biological imaging application: recent progress
380 and perspectives. *Mater. Today.* 2016;19(5):284-91.
- 381 [9] Mei J, Huang Y, Tian H. Progress and Trends in AIE-Based Bioprobes: A Brief Overview. *ACS*
382 *Appl. Mater. Interfaces.* 2018;10(15):12217-61.
- 383 [10] Gao H, Zhang X, Chen C, Li K, Ding D. Unity Makes Strength: How Aggregation-Induced
384 Emission Luminogens Advance the Biomedical Field. *Adv. Biosys.* 2018;2(9):1800074.

- 385 [11] Zhao Q, Chen Y, Liu Y. A polysaccharide/tetraphenylethylene-mediated blue-light emissive
386 and injectable supramolecular hydrogel. *Chin. Chem. Lett.* 2018;29(1):84-6.
- 387 [12] Yang Z, Chi Z, Mao Z, Zhang Y, Liu S, Zhao J, et al. Recent advances in mechano-responsive
388 luminescence of tetraphenylethylene derivatives with aggregation-induced emission properties.
389 *Mater. Chem. Front.* 2018;2(5):861-90.
- 390 [13] Wang J, Mei J, Hu R, Sun JZ, Qin A, Tang BZ. Click Synthesis, Aggregation-Induced
391 Emission, E/Z Isomerization, Self-Organization, and Multiple Chromisms of Pure Stereoisomers
392 of a Tetraphenylethylene-Cored Luminogen. *J. Am. Chem. Soc.* 2012;134(24):9956-66.
- 393 [14] Wu W, Ye S, Huang L, Xiao L, Fu Y, Huang Q, et al. A conjugated hyperbranched polymer
394 constructed from carbazole and tetraphenylethylene moieties: convenient synthesis through
395 one-pot "A₂ + B₄" Suzuki polymerization, aggregation-induced enhanced emission, and
396 application as explosive chemosensors and PLEDs. *J. Mater. Chem.* 2012;22(13):6374-82.
- 397 [15] Luo Q, Cao F, Xiong C, Dou Q, Qu D-H. Hybrid cis/trans Tetra-arylethenes with Switchable
398 Aggregation-Induced Emission (AIE) and Reversible Photochromism in the Solution, PMMA
399 Film, Solid Powder, and Single Crystal. *J. Org. Chem.* 2017;82(20):10960-7.
- 400 [16] Ozturk S, Atilgan S. A tetraphenylethylene based polarity dependent turn-on fluorescence
401 strategy for selective and sensitive detection of Hg²⁺ in aqueous medium and in living cells.
402 *Tetrahedron Lett.* 2014;55(1):70-3.
- 403 [17] Yuan Y, Zhang R, Cheng X, Xu S, Liu B. A FRET probe with AIEgen as the energy quencher:
404 dual signal turn-on for self-validated caspase detection. *Chem. Sci.* 2016;7(7):4245-50.
- 405 [18] Gu K, Qiu W, Guo Z, Yan C, Zhu S, Yao D, et al. An enzyme-activatable probe liberating
406 AIEgens: on-site sensing and long-term tracking of β -galactosidase in ovarian cancer cells. *Chem.*

- 407 Sci. 2019;10(2):398-405.
- 408 [19] Peng L, Zheng Y, Wang X, Tong A, Xiang Y. Photoactivatable Aggregation-Induced Emission
409 Fluorophores with Multiple-Color Fluorescence and Wavelength-Selective Activation. Chem. -
410 Eur. J. 2015;21(11):4326-32.
- 411 [20] Wang L, Li Y, You X, Xu K, Feng Q, Wang J, et al. An erasable photo-patterning material
412 based on a specially designed 4-(1,2,2-triphenylvinyl)aniline salicylaldehyde hydrazone
413 aggregation-induced emission (AIE) molecule. J. Mater. Chem. C. 2017;5(1):65-72.
- 414 [21] Yu CYY, Kwok RTK, Mei J, Hong Y, Chen S, Lam JWY, et al. A tetraphenylethene-based
415 caged compound: synthesis, properties and applications. Chem. Commun. 2014;50(60):8134-6.
- 416 [22] Wu B, Xue T, Wang W, Li S, Shen J, He Y. Visible light triggered aggregation-induced
417 emission switching with a donor-acceptor Stenhouse adduct. J. Mater. Chem. C.
418 2018;6(31):8538-45.
- 419 [23] Chevalier A, Renard P-Y, Romieu A. Azo-Based Fluorogenic Probes for Biosensing and
420 Bioimaging: Recent Advances and Upcoming Challenges. Chem. - Asian J. 2017;12(16):2008-28.
- 421 [24] Zhang J, Hu T, Liu Y, Ma Y, Dong J, Xu L, et al. Photoswitched Protein Adsorption on
422 Electrostatically Self-Assembled Azobenzene Films. ChemPhysChem. 2012;13(11):2671-5.
- 423 [25] Wang D, Wang X. Amphiphilic azo polymers: Molecular engineering, self-assembly and
424 photoresponsive properties. Prog. Polym. Sci. 2013;38(2):271-301.
- 425 [26] Ren H, Chen D, Shi Y, Yu H, Fu Z, Yang W. Charged End-Group Terminated
426 Poly(N-isopropylacrylamide)-b-poly(carboxylic azo) with Unusual Thermoresponsive Behaviors.
427 Macromolecules. 2018;51(9):3290-8.
- 428 [27] Wang G, Zhao XL, Zhao Y. Synthesis of azobenzene-containing liquid crystalline gelator for

- 429 use in liquid crystal gels. *Chin. Chem. Lett.* 2008;19(5):521-4.
- 430 [28] Lv J-a, Liu Y, Wei J, Chen E, Qin L, Yu Y. Photocontrol of fluid slugs in liquid crystal
431 polymer microactuators. *Nature.* 2016;537:179.
- 432 [29] Wang J, Wang S, Zhou Y, Wang X, He Y. Fast Photoinduced Large Deformation of Colloidal
433 Spheres from a Novel 4-arm Azobenzene Compound. *ACS Appl. Mater. Interfaces.*
434 2015;7(30):16889-95.
- 435 [30] Wang J, Wu B, Li S, Sinawang G, Wang X, He Y. Synthesis and Characterization of
436 Photoprocessable Lignin-Based Azo Polymer. *ACS Sustainable Chem. Eng.* 2016;4(7):4036-42.
- 437 [31] Yu X, Chen H, Shi X, Albouy P-A, Guo J, Hu J, et al. Liquid crystal gelators with
438 photo-responsive and AIE properties. *Mater. Chem. Front.* 2018;2(12):2245-53.
- 439 [32] Wang J, Wu B, Li S, He Y. NIR light and enzyme dual stimuli-responsive amphiphilic
440 diblock copolymer assemblies. *J. Polym. Sci., Part A: Polym. Chem.* 2017;55(15):2450-7.
- 441 [33] Li S, Wang J, Shen J, Wu B, He Y. Azo Coupling Reaction Induced Macromolecular
442 Self-Assembly in Aqueous Solution. *ACS Macro Lett.* 2018;7(4):437-41.
- 443 [34] Wu B, Wang W, Wang J, Li S, He Y. Redox triggered aggregation induced emission (AIE)
444 polymers with azobenzene pendants. *Dyes and Pigments.* 2018;157:290-7.
- 445 [35] Ye G, Qu X, Wang X, Bai Y, He Y, Wu B, et al. Epoxy-based Polymer Containing
446 Imidazole-type Azo Chromophores for Integrated Waveguide Applications. *J. Macromol. Sci., Part*
447 *A: Pure Appl.Chem.* 2010;47(12):1167-71.

Highlights

1. Imidazole-type azo caged aggregation-induced emission polymers were synthesized.
2. Only a small amount of imidazole-type azo groups could totally cage the strong AIE fluorescence of the polymers.
3. Imidazole-type azo chromophores of the polymers could be photo bleached with visible light, leading to activating their fluorescence performance.
4. Visible light induced fluorescent patterns have been easily fabricated and erased.